Proceedings of the ASME 2012 International Design Engineering Technical Conferences & Computers and Information in Engineering Conference
IDETC/CIE 2012
August 12-15, 2012, Chicago, IL, USA

DETC2012-70486

LINEAR CONTROL TECHNIQUES APPLIED TO THE OMNICOPTER MAV IN FIXED VERTICAL DUCTED FAN ANGLE CONFIGURATION

Yangbo Long, Sean Lyttle, David J. Cappelleri*
Multi-Scale Robotics and Automation Laboratory
Department of Mechanical Engineering
Stevens Institute of Technology
Hoboken, NJ 07030
Email: {ylong1, slyttle, David.Cappelleri} @stevens.edu

ABSTRACT

In this paper, linear control techniques are applied to a novel Omnicopter MAV design. This design is unique in its ability to withstand external disturbance and translate horizontally with more stable attitude. A dynamic model of the Omnicopter MAV has been developed using the Newton-Euler formalism. Based on a linearized version of the model with a fixed vertical ducted fan angle configuration, three different control schemes, namely PD control, Lyapunov-based control and optimal LQ control have been designed and proposed. Comparisons and relations between the three control schemes are discussed and simulations are presented. Finally, details on the Omnicopter prototype and initial test flights are presented. Controlled flights with vertical take-offs and landings have been achieved utilizing the PD control scheme.

I. INTRODUCTION

Autonomous micro aerial vehicles (MAV) can be used in tasks such as search and rescue, surveillance, building exploration, inspection and mapping. The MAV in the quadrotor configuration is based on the VTOL (Vertical Take-Off and Landing) concept and is viewed as an ideal platform to develop control laws, due to its simple structure, agility and controllability. In the last few years, the quadrotor MAV has been highlighted in many papers [1–6]. There has also been some recent work on unique MAV configurations that use gyroscopic moments for attitude control [7–9], MAVs in the tri-coptor [10–12] configurations, and coaxial MAVs [13, 14].

In this paper, we first review our novel VTOL MAV design called the *Omnicopter* (Fig. 1, top) [15]. Then we derive its dynamic model based on the Newton-Euler formalism, alternatively to the Euler-Lagrange method we used before. Next, we examine three different control schemes (PD, Lyapunov's direct method and optimal control) for a special operating case of the Omnicopter. Finally, we present a constructed prototype along with initial test flight results.

II. OMNICOPTER DESIGN OVERVIEW

A schematic of the Omnicopter configuration MAV is shown in Fig. 1 [15]. Drawing inspiration from omnidirectional wheels, the Omnicopter design allows for agile movements in any planar direction with fixed (zero) yaw, pitch and roll angles. It has five propellers: two fixed major coaxial counter-rotating propellers in the center used to provide most of the thrust and adjust the yaw angle, and three adjustable angle small ducted fans located in three places surrounding the airframe to control its roll and pitch. The Omnicopter has three main advantages over other VTOL UAVs, such as quadrotors and helicopters. First, the Omnicopter can generate roll and pitch motions two ways: M1: Fixed ducted fan angles with varying speeds; M2: Variable ducted fan angles and variable speeds. Second, all rotors are enclosed within pro-

*Address all correspondence to this author.

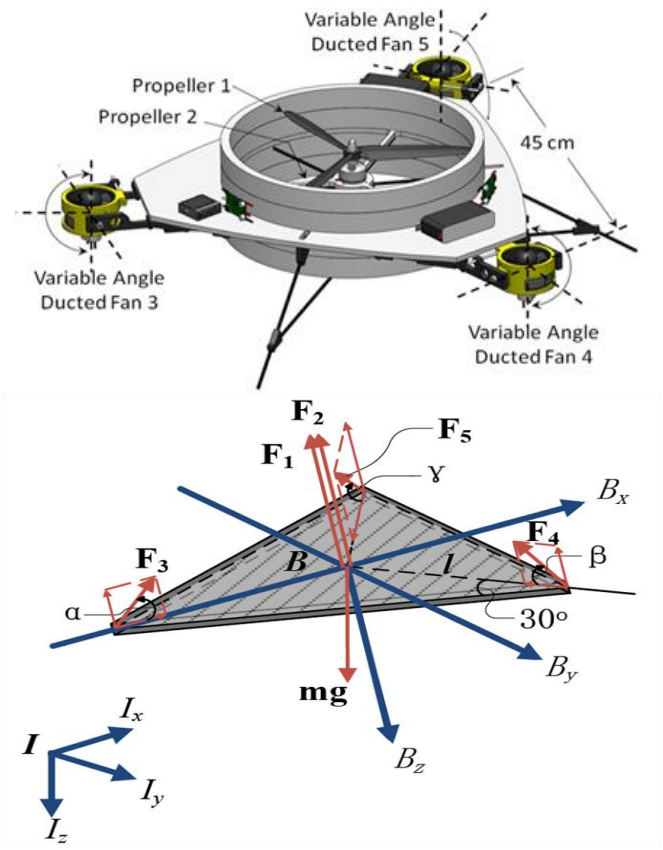

FIGURE 1. Omnicopter MAV Schematic (Top), and Omnicopter MAV free body diagram (Bottom), B: Body-fixed coordinate frame; I: Inertial reference frame.

tective ducts, permitting flights in obstacle-dense environments with reduced risk of damage. Third, the Omnicopter can maintain zero roll and pitch attitude for hover and lateral translation in the presence of disturbances (wind). This permits more stabilized horizontal flights.

III. SYSTEM MODELING

The coordinate systems and free body diagram for the Omnicopter are shown in Fig. 1. The inertial frame $I = \{I_x, I_y, I_z\}$ is considered fixed with respect to the earth, with axis I_z pointing downward. Let $B = \{B_x, B_y, B_z\}$, which is attached to the center of mass of the Omnicopter MAV, be the body frame, where the B_x axis is in the forward flight direction, B_y is perpendicular to B_x and positive to the right in the body plane, whereas B_z is orthogonal to the plane formed by B_x and B_y and points vertically downwards during perfect hover. The airframe orientation is expressed by a rotation matrix $\boldsymbol{R}_{Rot}$: $B \rightarrow I$, which is given by [16]:

$$\boldsymbol{R}_{Rot} = \begin{bmatrix} c\psi c\theta & c\psi s\theta s\phi - s\psi c\phi & c\psi s\theta c\phi + s\psi s\phi \\ s\psi c\theta & s\psi s\theta s\phi + c\psi c\phi & s\psi s\theta c\phi - s\phi c\psi \\ -s\theta & c\theta s\phi & c\theta c\phi \end{bmatrix}$$

where $c = \cos$ and $s = \sin$.

The time derivatives of the roll (ϕ), pitch (θ) and yaw (ψ) angles can be expressed in the form

$$\begin{bmatrix} \dot{\phi} \\ \dot{\theta} \\ \dot{\psi} \end{bmatrix} = \begin{bmatrix} 1 & \sin\phi\tan\theta & \cos\phi\tan\theta \\ 0 & \cos\phi & -\sin\phi \\ 0 & \sin\phi\sec\theta & \cos\phi\sec\theta \end{bmatrix} \begin{bmatrix} \omega_x \\ \omega_y \\ \omega_z \end{bmatrix}$$

where $\boldsymbol{\omega} = [\omega_x\ \omega_y\ \omega_z]^T$ is the angular velocity in the body frame.

We choose a coordinate vector $\boldsymbol{q} = [\boldsymbol{\varepsilon}; \boldsymbol{\zeta}] = [\varepsilon_1\ \varepsilon_2\ \varepsilon_3\ \phi\ \theta\ \psi]^T$, where $\boldsymbol{\varepsilon} = [\varepsilon_1\ \varepsilon_2\ \varepsilon_3]^T$ represents the position of the Omnicopter mass center expressed in the inertial frame I, and $\boldsymbol{\zeta} = [\phi\ \theta\ \psi]^T$ is the Euler angles vector. The external forces exerting on the Omnicopter can be obtained as the following:

$$\boldsymbol{F} = \boldsymbol{R}_{Rot} \begin{bmatrix} k_{F_2}(\Omega_3^2 c\alpha - (\Omega_4^2 c\beta + \Omega_5^2 c\gamma)s30^\circ) \\ k_{F_2}(\Omega_5^2 c\gamma - \Omega_4^2 c\beta)c30^\circ \\ -k_{F_1}(\Omega_1^2 + \Omega_2^2) - k_{F_2}(\Omega_3^2 s\alpha + \Omega_4^2 s\beta + \Omega_5^2 s\gamma) \end{bmatrix} \quad (1)$$

where k_{F1} and k_{F2} are factors that relate the central two and surrounding three propellers' speeds to thrusts, respectively. The 30° angle in (1) is shown in Fig. 1, and Ω_i denotes each propeller's speed, i = 1, 2, $\cdots$, 5.

Unlike a quadrotor model, with the two extra force components in the B_xB_y plane, the Omnicopter can achieve more stabilized lateral flights. Also the ability of withstanding disturbances is improved. The system's singularity is obtained at the expense of redundant actuators. But considering that the increased payload capability and the better flight stability with the powerful and variable ducted fans, we have proposed the Omnicopter MAV as an alternative solution to small VTOL UAVs.

The external torque vector, $\boldsymbol{\tau} = [\tau_x\ \tau_y\ \tau_z]^T$, acting about the x, y and z axes in the body frame are:

$$\begin{aligned} \tau_x &= (F_5 s\gamma - F_4 s\beta) l c30^\circ + J_p \omega_y (\Omega_1 - \Omega_2) \\ \tau_y &= (F_4 s\beta + F_5 s\gamma) l s30^\circ - F_3 s\alpha l + J_p \omega_x (\Omega_2 - \Omega_1) \\ \tau_z &= k_M (\Omega_1^2 - \Omega_2^2) \end{aligned} \quad (2)$$

Using the Newton-Euler approach [17], we can derive the dynamics of a rigid body under external forces and torques applied to the rigid body:

$$\begin{bmatrix} m\boldsymbol{I}_{3\times3} & \boldsymbol{0} \\ \boldsymbol{0} & \boldsymbol{J} \end{bmatrix} \begin{bmatrix} \dot{\boldsymbol{V}} \\ \dot{\boldsymbol{\omega}} \end{bmatrix} + \begin{bmatrix} \boldsymbol{\omega} \times m\boldsymbol{V} \\ \boldsymbol{\omega} \times \boldsymbol{J}\boldsymbol{\omega} \end{bmatrix} = \begin{bmatrix} \boldsymbol{f} \\ \boldsymbol{\tau} \end{bmatrix} \quad (3)$$

where $\boldsymbol{V} = [V_1\ V_2\ V_3]^T$ is the linear velocity expressed in the body frame, $\boldsymbol{J}$ is the inertial matrix, and $\boldsymbol{f} = [f_x\ f_y\ f_z]^T$ is the force vector in the body frame.

We can expand (3) to obtain 6 independent equations of motions as the following:

$$\begin{aligned} &m[\dot{V}_1 - V_2\omega_z + V_3\omega_y + gs\theta] = f_x \\ &m[\dot{V}_2 - V_3\omega_x + V_1\omega_z - gc\theta s\phi] = f_y \\ &m[\dot{V}_3 - V_1\omega_y + V_2\omega_x - gc\theta c\phi] = f_z \\ &I_{xx}\dot{\omega}_x - (I_{yy} - I_{zz})\omega_y\omega_z = \tau_x \\ &I_{yy}\dot{\omega}_y - (I_{zz} - I_{xx})\omega_x\omega_z = \tau_y \\ &I_{zz}\dot{\omega}_z - (I_{xx} - I_{yy})\omega_x\omega_y = \tau_z \end{aligned} \tag{4}$$

Using the Newton-Euler method, we derived the dynamical model in the body coordinate frame, as shown in (4). We can find that the translational equations of motion expressed in the body-fixed coordinate frame are pretty complex. Therefore, we prefer to express them in the inertial frame, while the rotational equations are expressed in the body-fixed frame (τ_x, τ_y and τ_z in (4)). Finally, the equations of motion are obtained as the following:

$$\begin{aligned} &\dot{\boldsymbol{\varepsilon}} = \boldsymbol{\upsilon} \\ &m\dot{\boldsymbol{\upsilon}} = mg\boldsymbol{e}_3 + \boldsymbol{F} \\ &\dot{\boldsymbol{R}}_{Rot} = \boldsymbol{R}_{Rot} \cdot sk(\boldsymbol{\omega}) \\ &\boldsymbol{J}\dot{\boldsymbol{\omega}} = -\boldsymbol{\omega} \times \boldsymbol{J}\boldsymbol{\omega} + \boldsymbol{\tau} \end{aligned} \tag{5}$$

where $\boldsymbol{\upsilon}$ is the velocity in the inertial frame, $\boldsymbol{e}_3 = [0\ 0\ 1]^T$, and

$$sk(\boldsymbol{\omega}) = \begin{bmatrix} 0 & -\omega_z & \omega_y \\ \omega_z & 0 & -\omega_x \\ -\omega_y & \omega_x & 0 \end{bmatrix}$$

In this paper, since we assume that the surrounding ducted fans point vertically upwards, the angles α, β and γ in (1) become 90°. In this case, the equations of motion of the translational subsystem will become

$$\begin{aligned} &m\ddot{\varepsilon}_1 = -(c\psi s\theta c\phi + s\psi s\phi)U_1 \\ &m\ddot{\varepsilon}_2 = -(s\psi s\theta c\phi - c\psi s\phi)U_1 \\ &m\ddot{\varepsilon}_3 - mg = -c\theta c\phi U_1 \end{aligned}$$

where $U_1 = k_{F_1}(\Omega_1^2 + \Omega_2^2) + k_{F_2}(\Omega_3^2 + \Omega_4^2 + \Omega_5^2)$.

IV. CONTROL DESIGN

The Omnicopter is controlled by nested feedback loop as shown in Fig. 2. The inner attitude control loop uses real-time Euler angles and angular speeds in the body frame from the IMU

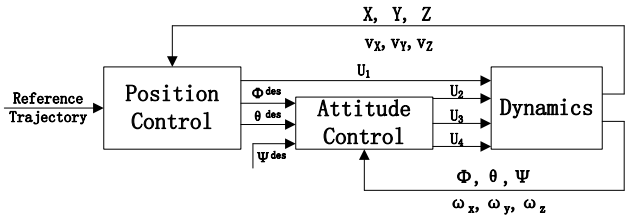

FIGURE 2. The nested control loops for position and attitude control

to control the roll, pitch and yaw, while the outer position control loop uses position and velocity of the robot in the inertial frame to control the trajectory in 3D. Similar nesting of control loops can be found in previous works [1, 2]. We developed three different control schemes for the Omnicopter, that is, the classical PD control, Lyapunov-based control and optimal LQ control, as presented now.

A. Classical PD Control Design

Attitude Control. We now present an attitude controller to follow the desired attitude generated by the position control loop. From (5), the attitude dynamics can be rewritten as

$$\begin{aligned} &\dot{\omega}_x = a_1\omega_y\omega_z + b_1U_2 \\ &\dot{\omega}_y = a_2\omega_x\omega_z + b_2U_3 \\ &\dot{\omega}_z = a_3\omega_x\omega_y + b_3U_4 \end{aligned}$$

where

$$\begin{aligned} &U_2 = k_{F_2}(\Omega_5^2 - \Omega_4^2) \\ &U_3 = k_{F_2}[(\Omega_4^2 + \Omega_5^2)\sin 30^\circ - \Omega_3^2] \\ &U_4 = k_M(\Omega_1^2 - \Omega_2^2) \end{aligned}$$

and $a_1 = \frac{I_{yy}-I_{zz}}{I_{xx}}$, $a_2 = \frac{I_{zz}-I_{xx}}{I_{yy}}$, $a_3 = \frac{I_{xx}-I_{yy}}{I_{zz}}$, $b_1 = \frac{l\cos 30^\circ}{I_{xx}}$, $b_2 = \frac{l}{I_{yy}}$, $b_3 = \frac{1}{I_{zz}}$.

If we apply the small angle approximation, $\phi \approx 0$ and $\theta \approx 0$, the relation between Euler angles' time derivatives and body angular speeds can be simplified to be

$$\begin{bmatrix} \dot{\phi} \\ \dot{\theta} \\ \dot{\psi} \end{bmatrix} = \begin{bmatrix} \omega_x \\ \omega_y \\ \omega_z \end{bmatrix}$$

Then the attitude subsystem can be linearized to be

$$\begin{aligned} &\ddot{\phi} = b_1U_2 \\ &\ddot{\theta} = b_2U_3 \\ &\ddot{\psi} = b_3U_4 \end{aligned} \tag{6}$$

Upon the above linear equation (6), we can design a PD controller for the attitude subsystem of the Omnicopter. The controls are given by:

$$\begin{aligned} U_2 &= K_{P2}(\phi^{des} - \phi) - K_{D2}\omega_x \\ U_3 &= K_{P3}(\theta^{des} - \theta) - K_{D3}\omega_y \\ U_4 &= K_{P4}(\psi^{des} - \psi) - K_{D4}\omega_z \end{aligned} \tag{7}$$

Position Control. As we have derived before, the position dynamics is shown as follows:

$$\begin{aligned} m\ddot{\varepsilon}_1 &= -(c\psi s\theta c\phi + s\psi s\phi)U_1 \\ m\ddot{\varepsilon}_2 &= -(s\psi s\theta c\phi - c\psi s\phi)U_1 \\ m\ddot{\varepsilon}_3 - mg &= -c\theta c\phi U_1 \end{aligned}$$

In the hover state, U_1 = mg, and under the small angle approximation, we obtain

$$\begin{aligned} m\ddot{\varepsilon}_1^{des} &= -(c\psi^{des}\theta^{des} + s\psi^{des}\phi^{des})mg \\ m\ddot{\varepsilon}_2^{des} &= -(s\psi^{des}\theta^{des} - c\psi^{des}\phi^{des})mg \end{aligned}$$

Therefore,

$$\begin{aligned} \ddot{\varepsilon}_1^{des} &= -g(\cos\psi^{des}\theta^{des} + \sin\psi^{des}\phi^{des}) \\ \ddot{\varepsilon}_2^{des} &= -g(\sin\psi^{des}\theta^{des} - \cos\psi^{des}\phi^{des}) \end{aligned}$$

If we assume the desired yaw angle ψ^{des} = 0, then from the above equations, we can get

$$\begin{aligned} \theta^{des} &= -\tfrac{1}{g}\ddot{\varepsilon}_1^{des} \\ \phi^{des} &= \tfrac{1}{g}\ddot{\varepsilon}_2^{des} \end{aligned}$$

The desired accelerations, $\ddot{\varepsilon}_i^{des}$ (i = 1, 2), are calculated from PD feedback of the position error, $e_i = (\varepsilon_{i,T} - \varepsilon_i)$, as

$$(\ddot{\varepsilon}_{i,T} - \ddot{\varepsilon}_i^{des}) + k_{d,i}(\dot{\varepsilon}_{i,T} - \dot{\varepsilon}_i) + k_{p,i}(\varepsilon_{i,T} - \varepsilon_i) = 0$$

where $\dot{\varepsilon}_{i,T} = \ddot{\varepsilon}_{i,T} = 0$ for hover, while for trajectory tracking control the reference velocity $\dot{\varepsilon}_{i,T}$ and reference acceleration $\ddot{\varepsilon}_{i,T}$ are calculated from time derivatives of reference trajectory $\varepsilon_{i,T}$.

On the other hand, the altitude dynamic equation, $m\ddot{\varepsilon}_3$ - mg = $-c\theta c\phi U_1$, is linearized to be

$$\ddot{\varepsilon}_3 = g - \tfrac{1}{m}U_1$$

So we can design a PD controller to control the altitude channel as well:

$$U_1 = mg + K_{P1}(\varepsilon_{3,d} - \varepsilon_3) + K_{D1}\frac{d(\varepsilon_{3,d} - \varepsilon_3)}{dt} \tag{8}$$

B. Control Design based on Lyapunov's Direct Method

In [18], the author used the Lyapunov's direct method to control the attitude subsystem of a quadrotor. Here we extend this method to control both the position and attitude systems. As we have derived in the PD control design, the linearized system is

$$\begin{aligned} \ddot{\varepsilon}_1 &= -g(\cos\psi^{des}\theta^{des} + \sin\psi^{des}\phi^{des}) \\ \ddot{\varepsilon}_2 &= -g(\sin\psi^{des}\theta^{des} - \cos\psi^{des}\phi^{des}) \\ \ddot{\varepsilon}_3 &= g - \tfrac{1}{m}U_1 \\ \ddot{\phi} &= b_1 U_2 \\ \ddot{\theta} &= b_2 U_3 \\ \ddot{\psi} &= b_3 U_4 \end{aligned} \tag{9}$$

We can choose state variables and make the following coordinate transformations:

$$\begin{aligned} x_1 &= \varepsilon_1 - \varepsilon_1^{des} & x_7 &= \phi - \phi^{des} \\ x_2 &= \dot{\varepsilon}_1 & x_8 &= \omega_x \\ x_3 &= \varepsilon_2 - \varepsilon_2^{des} & x_9 &= \theta - \theta^{des} \\ x_4 &= \dot{\varepsilon}_2 & x_{10} &= \omega_y \\ x_5 &= \varepsilon_3 - \varepsilon_3^{des} & x_{11} &= \psi - \psi^{des} \\ x_6 &= \dot{\varepsilon}_3 & x_{12} &= \omega_z \end{aligned} \tag{10}$$

Position Control. First, let's construct a candidate Lyapunov function, V_1, which is a positive definite function around the origin:

$$V_1 = \frac{1}{2}(k_1x_1^2 + x_2^2 + k_2x_3^2 + x_4^2 + k_3x_5^2 + x_6^2)$$

Using equations (9) and (10), the time derivative of V_1 can be calculated to be

$$\begin{aligned} \dot{V}_1 = k_1x_1x_2 + x_2[-g(\cos\psi^{des}\theta^{des} + \sin\psi^{des}\phi^{des})] + k_2x_3x_4 + \\ x_4[-g(\sin\psi^{des}\theta^{des} - \cos\psi^{des}\phi^{des})] + k_3x_5x_6 + x_6(g - \tfrac{1}{m}U_1) \end{aligned} \tag{11}$$

Therefore, we can simply choose the virtual control inputs ϕ^{des}, θ^{des} and the control input U_1 to be

$$\begin{aligned} \phi^{des} &= -\tfrac{\sin\psi^{des}}{g}(-k_1x_1 - k_4x_2) + \tfrac{\cos\psi^{des}}{g}(-k_2x_3 - k_5x_4) \\ \theta^{des} &= -\tfrac{\cos\psi^{des}}{g}(-k_1x_1 - k_4x_2) - \tfrac{\sin\psi^{des}}{g}(-k_2x_3 - k_5x_4) \\ U_1 &= m(g + k_3x_5 - k_6x_6) \end{aligned} \tag{12}$$

After substituting (12) into (11) and with k_i (i = 1, 2, ..., 6) as positive constants, we obtain

$$\dot{V}_1 = -k_4x_2^2 - k_5x_4^2 - k_6x_6^2$$

which is negative semi-definite. Since the set $S = \{\dot{V}_1 = 0\}$ is restricted only to the origin $x_i = 0$ (i = 1, 2, ..., 6), by LaSalle invariance theorem, we can ensure the asymptotic stability of the system.

Attitude Control. Next, for the attitude control design, we construct another candidate Lyapunov function V_2:

$$V_2 = \frac{1}{2}(k_7 x_7^2 + x_8^2 + k_8 x_9^2 + x_{10}^2 + k_9 x_{11}^2 + x_{12}^2)$$

Using equations (9) and (10), the time derivative of V_2 can be calculated to be

$$\dot{V}_2 = k_7 x_7 x_8 + x_8 b_1 U_2 + k_8 x_9 x_{10} + x_{10} b_2 U_3 + k_9 x_{11} x_{12} + x_{12} b_3 U_4 \tag{13}$$

Therefore, we can choose the control inputs U_2, U_3 and U_4 to be

$$\begin{aligned} U_2 &= \tfrac{1}{b_1}(-k_7 x_7 - k_{10} x_8) \\ U_3 &= \tfrac{1}{b_2}(-k_8 x_9 - k_{11} x_{10}) \\ U_4 &= \tfrac{1}{b_3}(-k_9 x_{11} - k_{12} x_{12}) \end{aligned} \tag{14}$$

After substituting (14) into (13) and with k_i (i = 7, 8, ..., 12) as positive constants, we obtain

$$\dot{V}_2 = -k_{10} x_8^2 - k_{11} x_{10}^2 - k_{12} x_{12}^2$$

In the same way, the asymptotic stability can be guaranteed.

We can find that essentially the control inputs designed using Lyapunov direct method are similar to those found using PD control, although the control design process is different. Therefore, we can tune the control parameters in the Lyapunov-based design by following the same procedure in the PD control design. The controls' performances in both designs should be close to each other with proper tuning.

C. Optimal Control Design

For the linearized attitude subsystem (6), we can describe it in the state space as:

$$\dot{\boldsymbol{x}} = \boldsymbol{A}\boldsymbol{x} + \boldsymbol{B}\boldsymbol{u}$$

where $\boldsymbol{x} = [\phi\ \dot{\phi}\ \theta\ \dot{\theta}\ \psi\ \dot{\psi}]^T$ and $\boldsymbol{u} = [U_2\ U_3\ U_4]^T$.

We can also control the linearized attitude subsystem using optimal LQ control. In order to apply the LQ control, let's define the cost functional to be:

$$J_C = \int (\boldsymbol{x}^T \boldsymbol{Q} \boldsymbol{x} + \boldsymbol{u}^T \boldsymbol{R} \boldsymbol{u}) dt$$

The feedback control law that minimizes the cost value is:

$$\boldsymbol{u} = -\boldsymbol{K_c}\boldsymbol{x} \tag{15}$$

where the LQR control gain matrix $\boldsymbol{K_c}$ is provided by $\boldsymbol{K_c} = \boldsymbol{R}^{-1}\boldsymbol{B}^T\boldsymbol{P}$, and $\boldsymbol{P}$ is derived by solving the algebraic Riccati equation:

$$-\boldsymbol{P}\boldsymbol{A} - \boldsymbol{A}^T\boldsymbol{P} + \boldsymbol{P}\boldsymbol{B}\boldsymbol{R}^{-1}\boldsymbol{B}^T\boldsymbol{P} - \boldsymbol{Q} = \dot{\boldsymbol{P}}$$

The control output and the Omnicopter behavior are tuned by varying matrices $\boldsymbol{Q}$ and $\boldsymbol{R}$. The matrices are chosen to be symmetric and positive-definite. A first choice for the matrices $\boldsymbol{Q}$ and $\boldsymbol{R}$ is given by the Bryson's rule [19]:

$$\begin{aligned} \boldsymbol{Q}_{ii} &= \frac{1}{\textit{maximum acceptable value of state } i} \\ \boldsymbol{R}_{jj} &= \frac{1}{\textit{maximum size of control input } j} \end{aligned}$$

The weighting matrices $\boldsymbol{Q}$ and $\boldsymbol{R}$ are used to give different emphases to different states and control inputs. The magnitude of the $\boldsymbol{Q}$ matrix minimizes the error of states, and the $\boldsymbol{R}$ matrix minimizes the energy consumption of control. For this linearized plant, the control gain $\boldsymbol{K_c}$ is designed with the following weighting matrices:

$$\boldsymbol{Q} = \begin{bmatrix} 1 & 0 & 0 & 0 & 0 & 0 \\ 0 & 0.001 & 0 & 0 & 0 & 0 \\ 0 & 0 & 1 & 0 & 0 & 0 \\ 0 & 0 & 0 & 0.001 & 0 & 0 \\ 0 & 0 & 0 & 0 & 1 & 0 \\ 0 & 0 & 0 & 0 & 0 & 0.001 \end{bmatrix}$$

and $\boldsymbol{R} = 0.01 * \boldsymbol{I}_{3x3}$.

So that

$$\boldsymbol{K_c} = \begin{bmatrix} 10 & 2.9846 & 0 & 0 & 0 & 0 \\ 0 & 0 & 10 & 3.1560 & 0 & 0 \\ 0 & 0 & 0 & 0 & 10 & 1.7550 \end{bmatrix}$$

The substitution of the gain matrix $\boldsymbol{K_c}$ into (15) leads us to conclude that the LQR controller is essentially a PD controller as well. This is expected because when using optimal control, the closed-loop poles of the linear system are automatically dictated by the weighting matrices $\boldsymbol{Q}$ and $\boldsymbol{R}$, while the pole assignment is equivalent to the PD control in the form of controllers. Consequently, it serves as another way to help tune the PD control gains.

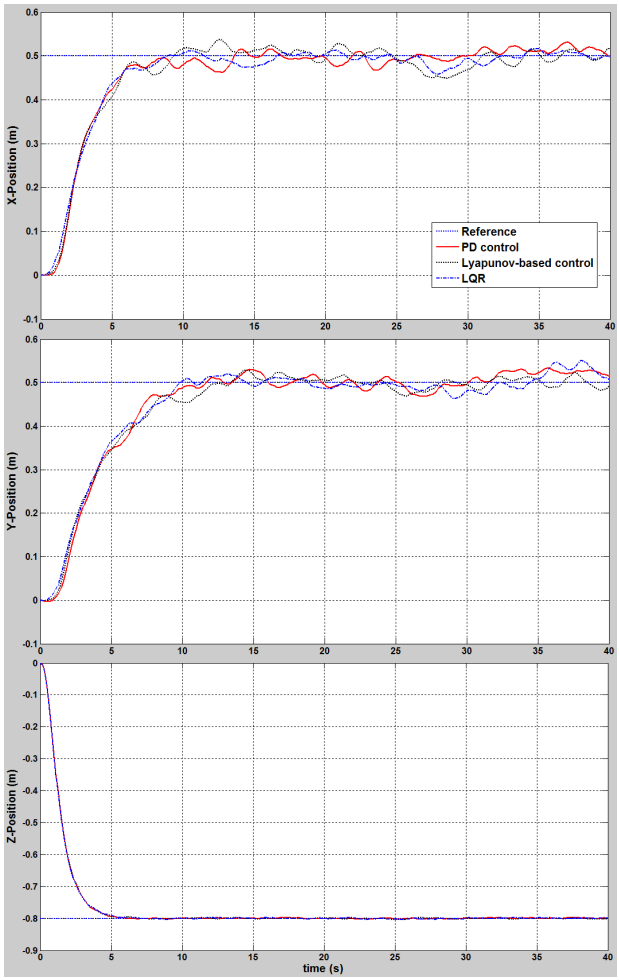

FIGURE 3. Point-to-point movement control of the Omnicopter MAV with noise and disturbances: moving from (0, 0, 0) to (0.5, 0.5, -0.8) m

V. SIMULATION RESULTS

Based on the control designs discussed above, simulations are done for the Omnicopter. The point-to-point movement is simulated as shown in Fig. 3. Since the model is built in a North-East-Down frame, Z = -0.8 m in Fig. 3 means that the flying height is 0.8 m. To make the simulations more realistic, random white noise with zero mean and 0.01 variance have been added to the position and velocity measurements, and the attitude and angular velocity have been corrupted by noise with 0.0001 variance.

In the first simulation, the Omnicopter was tasked to perform a point-to-point movement. In this simulation, besides the white noise mentioned above, periodic disturbances have also been added to the dynamical model as the following:

$$\boldsymbol{d}_1 = \begin{bmatrix} 0.1\sin(\pi t) + 0.1\sin(\pi t/10) \\ 0.1\sin(\pi t) + 0.1\sin(\pi t/10) \\ 0.1\sin(\pi t) + 0.1\sin(\pi t/10) \end{bmatrix} * 10^{-1} N$$

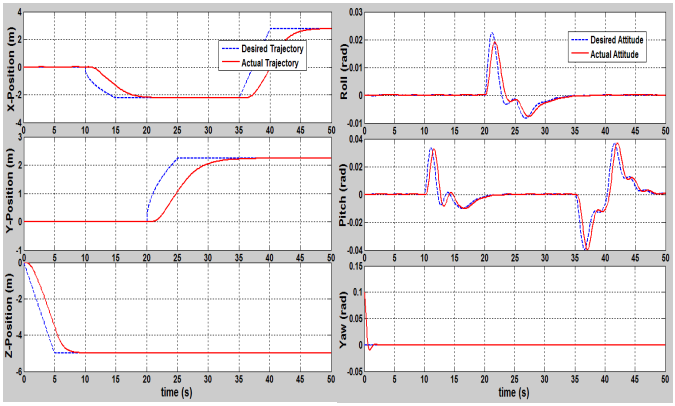

FIGURE 4. PD control: position and attitude (trajectory tracking)

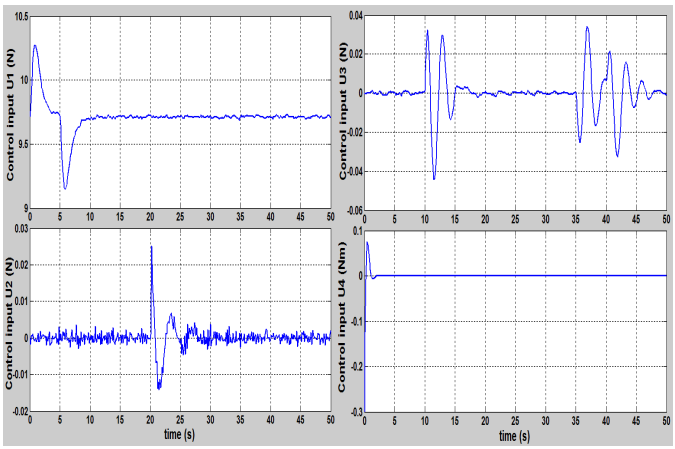

FIGURE 5. PD control: control inputs (trajectory tracking)

and

$$\boldsymbol{d}_2 = \begin{bmatrix} 0.1\sin(\pi t) + 0.1\sin(\pi t/10) \\ 0.1\sin(\pi t) + 0.1\sin(\pi t/10) \\ 0.1\sin(\pi t) + 0.1\sin(\pi t/10) \end{bmatrix} * 10^{-2} N \cdot m$$

Then the dynamical model with external disturbances can be rewritten to be:

$$\begin{aligned} \dot{\boldsymbol{\varepsilon}} &= \boldsymbol{v} \\ m\dot{\boldsymbol{v}} &= mg\boldsymbol{e}_3 + \boldsymbol{R}_{Rot}\boldsymbol{f} + \boldsymbol{d}_1 \\ \dot{\boldsymbol{R}}_{Rot} &= \boldsymbol{R}_{Rot} \cdot sk(\boldsymbol{\omega}) \\ \boldsymbol{J}\dot{\boldsymbol{\omega}} &= -\boldsymbol{\omega} \times \boldsymbol{J}\boldsymbol{\omega} + \boldsymbol{\tau} + \boldsymbol{d}_2 \end{aligned} \tag{16}$$

As we have discussed above, the form of controllers designed in three different ways is essentially the same. So the control performance of them should be close to each other, as long as the control gains are tuned properly. As shown in Fig. 3,

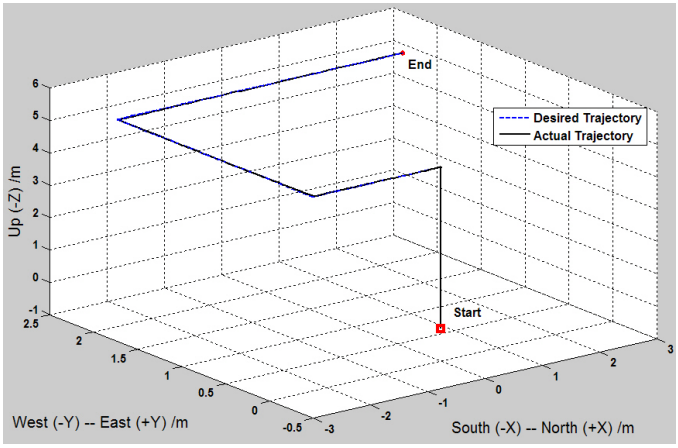

FIGURE 6. PD control: 3D trajectory tracking of the Omnicopter MAV with noise

the position responses of the closed loop system using the controllers designed in three different ways are almost identical.

In the second simulation, the control objective was to make the aircraft track a 3D trajectory in the presence of random white noise. Fig. 4 - 6 show the position, attitude, control inputs and 3D tracking performance for the PD controller case. These results prove the effectiveness of the proposed PD controller.

VI. PROTOTYPE CONSTRUCTION AND TESTS

A. Prototype Construction

An Omnicopter prototype in the fixed vertical ducted fan angle configuration has been constructed, as shown in Fig. 7. The skeleton of the airframe is made from 0.125" diameter carbon fiber rods along with custom connecting joints laser cut from ABS plastic. The body of the Omnicopter is made from Deprom 6 mm thick hobby foam that was similarly laser cut to size. The two center propellers are 10 x 7 3-blade Maser Airscrew propellers from Windsor Propeller Company, Inc. (*masterairscrew.com*). They are attached to two BP-U2212/10 brushless outrunner motors from BP Hobbies LLC (*www.bphobbies.com*) which are controlled with two Thunderbird brushless 18 Amp electronic speed controllers (ESCs) from Castle Creations, Inc. (*www.castlecreations.com*). The three ducted fans are 50 mm EDF (electric ducted fans) from *Toysonics.com* operating on three Great Planes Speed 120 brushed motors (*www.greatplanes.com*) with Blue Arrow 10A brushed ESCs (*www.bluearrow-rc.com*). Custom mounts for each of the ducted fans were 3D printed out of ABS plastic. The Omnicopter uses the ArduPilotMega from 3D Robotics (*3Drobotics.com*) for an IMU and on-board control. A XBee transceiver module allows for wireless data logging of the IMU data on a local PC. The entire system is powered with two Thunderpower 3-cell 1350 mAhr Lithium Polymer batteries (*www.thunderpowerrc.com*). The prototype weighs 2 lbs 3.5 oz. with an available payload at 80% power of approximately 2 lbs 6 oz (∼1 kg). This initial prototype is currently configured for remote control with a Spektrum AR8000 8-Channel DSMX Receiver and DX8 8-channel transmitter (*www.spektrumrc.com*).

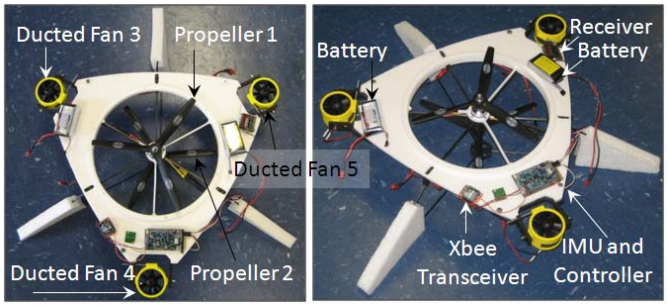

FIGURE 7. Omnicopter prototype: Top View (left) and Isometric View (right)

B. Preliminary Test Flights

In order to implement the controller, we have to transform the controls proportional to force/torques into rotor speeds, which are in turn transformed into supply voltages. The relation between the controls and rotor speeds is as follows:

$$
\begin{aligned}
U_1 &= k_{F_1}(\Omega_1^2+\Omega_2^2)+k_{F_2}(\Omega_3^2+\Omega_4^2+\Omega_5^2)\\
U_2 &= k_{F_2}(\Omega_5^2-\Omega_4^2)\\
U_3 &= k_{F_2}[(\Omega_4^2+\Omega_5^2)\sin 30^\circ-\Omega_3^2]\\
U_4 &= k_M(\Omega_1^2-\Omega_2^2)
\end{aligned}
$$

With Ω_3 being a known value which can be assigned as we want, we can solve the above equations and arrive at desired rotor speeds. Initial test flights of the system are underway. Manual remote control of the lift propellers and robot position has been coupled with a PD attitude controller. Vertical takeoffs and landings have been achieved with the PD stabilized attitude control, as shown in Fig. 8.

VII. CONCLUSION

In this paper, we studied the control problem of a new configuration of a MAV called the Omnicopter. It has some advantages over comparable VTOL UAVs with regard to its ability to produce lateral force vectors. We have presented a dynamic model of the Omnicopter using the Newton-Euler formalism. In the initial phase of study, we start from studying the control problem of the Omnicopter in fixed vertical ducted fan angle configuration. For this particular configuration, three different control designs are presented and analyzed, along with simulations. We

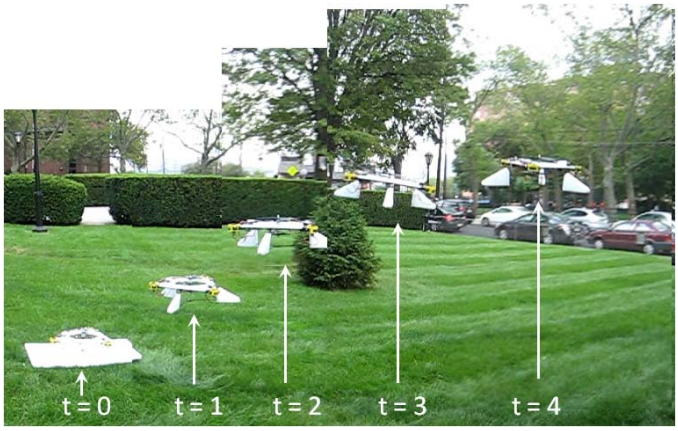

FIGURE 8. Image mosaic of a preliminary test flight of the Omnicopter

found that for the linearized model, the controllers we finally arrived at will be essentially the same. Thus we implemented the PD control on the prototype we built. Initial test flights show that the attitude controller can stabilize the Omnicopter well.

Future work will essentially investigate the more advanced control method (M2), that is, controlling it by varying both angles and speeds of the ducted fans, for increased performance. Autonomous operation in cluttered environments through accurate trajectory control using linear and/or nonlinear control techniques will also be explored in the next phase.

REFERENCES

[1] Bouabdallah, S., Noth, A., and Siegwart, R., 2004. "Pid vs lq control techniques applied to an indoor micro quadrotor". *Proc. IEEE int. conf. on intelligent robots and systems,* ***3***, pp. 2451–2456.

[2] Michael, N., Mellinger, D., Lindsey, Q., and Kumar, V., Sept. 2010. "The grasp multiple micro uav testbed". *IEEE Robotics and Automation Magazine*.

[3] Hoffmann, G. M., Huang, H., Waslander, S. L., and Tomlin, C. J., 2011. "Precision flight control for a multi-vehicle quadrotor helicopter testbed". *Control Engineering Practice,* ***19:1023-1036***.

[4] Nicol, C., Macnab, C., and Ramirez-Serrano, A., 2011. "Robust adaptive control of a quadrotor helicopter". *Mechatronics,* ***21:927-938***.

[5] Bertrand, S., Guénard, N., Hamel, T., Piet-Lahanier, H., and Eck, L., 2011. "A hierarchical controller for miniature vtol uavs: Design and stability analysis using singular perturbation theory". *Control Engineering Practice,* ***19:1099-1108***.

[6] Alexis, K., Nikolakopoulos, G., and Tzes, A., 2011. "Switching model predictive attitude control for a quadrotor helicopter subject to atmospheric disturbances". *Control Engineering Practice,* ***19:1195-1207***.

[7] Gress, G., 2002. "Using dual propellers as gyroscopes for tilt-prop hover control". *In Proc. AIAA Biennial Int. Powered Lift Conf. Exhibit, Williamsburg, VA*.

[8] Lim, K., and Moerder, D., 2007. "Cmg-augmented control of a hovering vtol platform". *AIAA Guidance, Navigation, and Control Conference and Exhibit, Hilton Head, SC*, August.

[9] Thorne, C., and Yim, M., 2011. "Towards the development of gyroscopically controlled micro air vehicles". *International Conference on Robotics and Automation, Shanghai, China*, May.

[10] Escareno, J., Sanchez, A., Garcia, O., and Lozano, R., 2008. "Triple tilting rotor mini-uav: Modeling and embedded control of the attitude". *2008 American Control Conference*.

[11] Salazar-Cruz, S., Kendoul, F., Lozano, R., and Fantoni, I., 2006. "Real-time control of a small-scale helicopter having three rotors". *Proceedings of the 2006 IEEE/RSJ International Conference on Intelligent Robots and Systems*.

[12] Rongier, P., Lavarec, E., and Pierrot, F., 2005. "Kinematic and dynamic modeling and control of a 3-rotor aircraft". In Robotics and Automation, 2005. ICRA 2005. Proceedings of the 2005 IEEE International Conference on, pp. 2606 – 2611.

[13] Andersh, J., and Mettler, B., 2011. "System integration of a miniature rotorcraft for aerial tele-operation research". *Mechatronics,* ***21:776-788***.

[14] Schafroth, D., Bermes, C., Bouabdallah, S., and Siegwart, R., 2010. "Modeling, system identification and robust control of a coaxial micro helicopter". *Control Engineering Practice,* ***18:700-711***.

[15] Long, Y., Lyttle, S., Pagano, N., and Cappelleri, D. J., 2012. "Design and quaternion-based attitude control of the omnicopter mav using feedback linearization". *ASME International Design Engineering Technical Conference (IDETC)*.

[16] Spong, M. W., Hutchinson, S., and Vidyasagar, M., 2006. *Robotic Modeling and Control*. John Wiley & Sons, Inc., 111 River Street, Hoboken, NJ 07030-5774.

[17] Murray, R. M., Li, Z., and Sastry, S. S., 1994. *A Mathematical Introduction to Robotic Manipulation*. CRC Press, Boca Raton, FL.

[18] Bouabdallah, S., 2007. "Design and control of quadrotors with application to autonomous flying". PhD thesis, Ecole Polytechnique Fédérale de Lausanne (EPFL).

[19] Orsag, M., Poropat, M., and Bogdan, S., 2010. "Hybrid fly-by-wire quadrotor controller". *IEEE International Symposium on Industrial Electronics (ISIE), Bari, Italy*, July.